

SAXS Studies of Heating/Cooling Cycle Behavior of Biodegradable BTA/PLA-b Blends

Ryszard Kwiatkowski,^{*1} Piotr Dacko²

Summary: The blends of BTA copolyester (i.e. the Ecoflex[®] copolyester) and PLA-b amorphous polylactide with following weight ratios: 90/10, 70/30 and 50/50 have been prepared and their phase structure have determined by using X-ray methods and DSC method. The thermal behavior of the blends was tested by time resolved SAXS measurements performed during heating/cooling thermal cycle treatment (20÷135÷20 °C). As a result of analysis of desmeared Lorentz corrected SAXS curves using the Hosemann scattering function the changes of characteristics of lamellar structure of BT-BA stacks within the blends have been determined and linked with changes of lamellar superstructure of the BTA reference sample. Among other thinks, it was found that the rate of the heating induced growth of the BA amorphous layers thickness and consequently of long period of BT-BA stacks structure increases with the increase of PLA-b amount, and that BT-BA stacks are formed significantly later (ca. 5 min.) during the cooling of the melted blends than during the cooling of the melted BTA copolyester.

Keywords: biodegradable blends; BTA; SAXS; thermal properties; WAXS

Introduction

Biodegradable polymers are of great importance to modern science and the technology of polymer-based useful materials. They find extensive use in medicine, agriculture, and in the production of throw-away wrappings and goods. Unfortunately, specific properties of biodegradable polymers are a barrier to their use in some cases. For instance, glass transition at relatively high temperature considerably limits applications of PLA biopolymer (ca. 56 °C) because of its fragility at room temperature. To widen the range of possible applications of commercialized biodegradable polymer materials different modification methods can be applied. One, among others, is polymer blends preparation. This results in

structure modification and, consequently, in changes of blends behavior during e.g. thermoforming processes as compared with pure components of the blends. This work deals with the determination of both an extent and the rate of superstructure changes occurring during heating/cooling cycle treatment of biodegradable blends of aliphatic-aromatic copolyester (BTA) with the BASF trade mark Ecoflex[®] and amorphous polylactide (PLA-b) (PABR-L-68 polylactide; Galactic S.A.), with following weight ratios: BTA90wt/PLA10wt, BTA70wt/PLA30wt and BTA50wt/PLA50wt. For this purpose, time resolved SAXS measurements were performed during step-heating/continuous-cooling cycles (20 °C÷135 °C÷20 °C) of extruded BTA/PLA-b blends as well as for a reference sample of BTA copolyester prepared in the same conditions of extrusion.

Experimental Part

Samples

BTA/PLA-b mixtures were prepared by dissolution of initial polymers in chloro-

¹ University of Bielsko-Biala, Willowa 2, 43-309 Bielsko-Biala, Poland
Fax: (+48) 33 8279100;
E-mail: rkwiatkowski@ath.bielsko.pl

² Centre of Polymer and Carbon Materials, Polish Academy of Sciences, M.Curie-Skłodowska 34, 41-819 Zabrze, Poland

form (10% solution) and next precipitation in hexane (chloroform: hexane = 1: 3). Precipitated polymer mixtures were first dried at room temperature for 72 hours and finally dried under a vacuum at 40 °C for 96 hours. Dried polymer mixtures were extruded using the laboratory single-screw extruder (ZMP-W, Poland). Temperatures in each zone of the extruder changed from 60 °C in the supply zone to 120 °C in the flow zone, and 100 °C at the extrusion head.

Measurements and Data Treatment

Phase structure of the blends as prepared and of the reference samples, i.e. of extruded: BTA and PLA-b blends compounds was preliminarily tested by both WAXS and DSC methods.

The WAXD measurements were carried out on a Seifert URD 6 diffractometer equipped with a graphite monochromator and a Cu target sealed X-ray tube ($\lambda = 1.542 \text{ \AA}$). The step scanning mode was employed over a 2θ scattering angle ranging from 2° to 60° , with a step-size of 0.1° . The decomposition of WAXS patterns into diffraction components (i.e. diffraction peaks and diffuse maxima) was accomplished by means of a multi-Lorentz non-linear fit procedure as implemented in Microcal(TM) Origin[®] Version 7.5. This procedure results in: the position, the full width at half height and the area of diffraction components observed and a fitted curve (i.e. a superposition of the components).

DSC measurements were performed using sealed aluminum pans under nitrogen atmosphere at a rate of $10^\circ\text{C}/\text{min}$ from -60°C to $+200^\circ\text{C}$. TA-DSC 2010 system was employed.

Time resolved small angle X-ray scattering (SAXS) measurements were carried out on a compact Kratky camera equipped with a Hecus-MBraun optical system and a hot stage and KHR-300 temperature controller of Anton-Paar. A copper X-ray tube was used as the radiation source ($\text{CuK}\alpha$ $\lambda = 1.542 \text{ \AA}$) and the resolution of the detection system was ca. 800 \AA° . To determine the temperature of a sample during the real time of SAXS measurements, a self-prepared setup testing sample holder temperature was used since, as in the original equipment for temperature measurements on the Kratky camera heating temperature of the cuvette holder is controlled only. The setup consisted of: a thermocouple, a temperature multimeter and a computer registration system which enabled us to register sample holder temperature automatically during the heating/cooling cycle every 30 s, at a point as close as possible to the sample (see Figure 1). Changes in temperature of the sample during the cycle treatment applied are shown in Figure 2. The arrow capped horizontal lines in this figure indicate periods of SAXS measurements performed. From the T vs. t cooling curve (Figure 2 right side) the $\langle T \rangle$ means temperature of the sample at a given period of SAXS measurement was determined in accordance with the Eqs. 1.

$$\langle T \rangle = \frac{1}{\Delta} \int_{t_i}^{t_j} T(t) dt; \Delta t = t_j - t_i = 5 [\text{min}] \quad (1)$$

The SAXS patterns were analyzed using: 3DV Hecus and Microcal(TM) Origin[®]

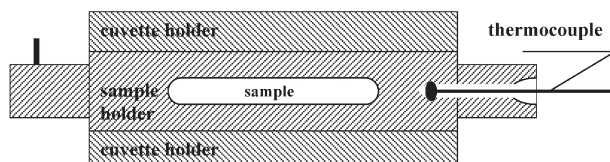


Figure 1.

The sketch of location of temperature testing point within a modified sample holder.

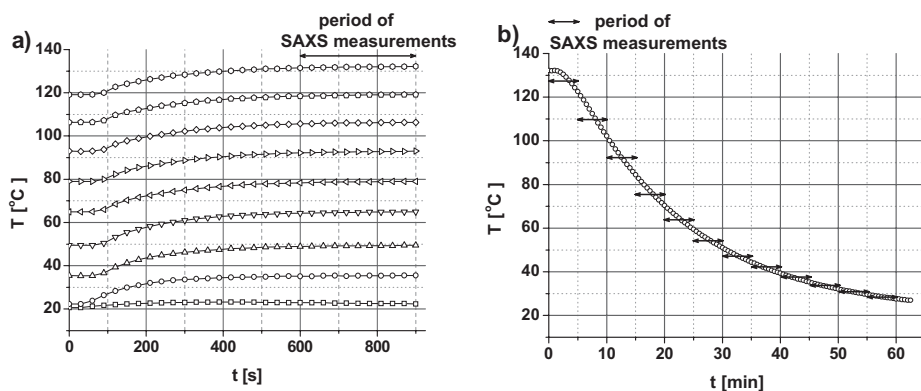


Figure 2.

The changes in temperature of the sample during the cycle treatment applied: a) step-heating; b) subsequent continuous-cooling.

Version 7.5 software. They were: desmeared^[1], corrected for background scattering^[2] ($I_B = F_{\text{exp}}(bq^2)$), and then converted to Lorentz corrected SAXS curves: $I(q)q^2$ vs. q , where $q = 4\pi \sin\theta/\lambda$ – the vector scattering magnitude (see Figure 4).

Finally, for each temperature of the cyclic treatment:

- experimental scattering power (Q_{exp}) of the sample has been determined in accordance with the equation^[3,4]:

$$Q_{\text{exp}} = \int_{q_2}^{q_1} I(q)q^2 dq; \quad 0.0085 \leq q \leq 0.535 \text{ \AA}^{-1} \quad (2)$$

- a mean thicknesses of flat lamellae constituted lamellar stacks as well as a mean long period of a lamellar superstructure have been determined as a result of nonlinear fitting of the Hosemann scattering function^[5,6] (Eqs. 3) to Lorentz corrected SAXS curves which exhibited a diffraction maximum.

$$I(q)q^2 \approx \frac{I_0}{q^2} \left\{ \frac{1 - A^2 B^2 - A(1 - B^2)\cos(q < d_1 >) - B(1 - A^2)\cos(q < d_2 >)}{1 + A^2 B^2 - 2AB\cos(q < d_1 > + q < d_2 >)} \right\} \quad (3)$$

where:

- $q = 4\pi \sin\theta/\lambda$
- σ_1 and σ_2 : standard deviation of Gaussian distribution of d_1 and d_2 thicknesses of flat

lamellae with an electron density contrast constituted lamellar stacks

- $\langle d_1 \rangle$ and $\langle d_2 \rangle$: mean thicknesses of flat lamellae
- $A = \exp(-q^2 \sigma_1/2)$ and $B = \exp(-q^2 \sigma_2/2)$
- $\langle L \rangle = \langle d_1 \rangle + \langle d_2 \rangle$: a mean long period of a lamellar superstructure

Results and Discussion

The WAXS patterns of reference samples, i.e. of the extruded: PLA-b polylactide and BTA copolyester are shown in Figure 3 along with their decomposition into diffraction components. In the case of the BTA reference sample the WAXS pattern consists of the indexed sharp diffraction peaks (the left side of Figure 3) originated in BT crystalline phase^[7,8,9,10,11] and diffuse scattering maxima (centered at: 20.1° and 42.6°) attributed to BA amorphous phase. The

WAXS derived crystallinity of the BTA reference sample, calculated as the ratio of the total area under the crystalline peaks to the total area of the diffraction pattern, amount to ca. 22%. In the case

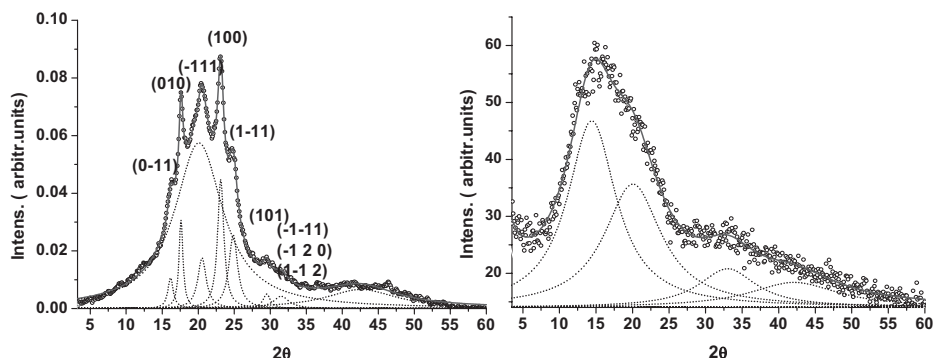


Figure 3.

The resolution of WAXS pattern of: BTA (left side) and PLA-b (right side) into diffraction components; ○ = experimental points; — = fitted curve; ● = Lorentz shaped diffraction components.

of the PLA-b reference sample the central part of diffraction pattern (right side of Figure 3) is in the shape of a complex asymmetrical diffusive maximum. In accord with the amorphous cell model of PLLA/PDLA's structure given by Blomqvist et al.^[12] three diffuse bends, centered at the 2θ scattering angles equaling ca.: 15° , 22° and 33° have been separated as diffraction components of the PLA-b WAXS pattern. The characteristics of the blends compounds wide-angle X-ray scattering are clearly recognizable in the WAXS patterns of the blends as prepared. The patterns are shown in Figure 4 left side.

First, there is a good agreement between WAXS diffraction peaks found for the BTA copolyester and diffraction peaks observed for the blends. Second, in the

range of 2θ from 10° to 15° a diffuse scattering maximum becomes stronger and stronger as PLA-b content in the blends increases. These observations indicated that both BT-BA semicrystalline domains and PLA-b amorphous domains occur separately within the BTA/PLA-b blends. The three phase structure of the blends has been confirmed as well by the DSC and the SAXS investigations. In accordance with DSC measurements (data is not presented) the blends exhibited: two glass transitions at: $T_g \approx -31^\circ\text{C}$ and $T_g \approx 56^\circ\text{C}$, and a single endothermic transition at $T_m \approx 132^\circ\text{C}$, i.e. at temperatures close to characteristic temperatures of phase transitions of the blends compounds.^[9] The SAXS measurements at ambient temperature revealed (see

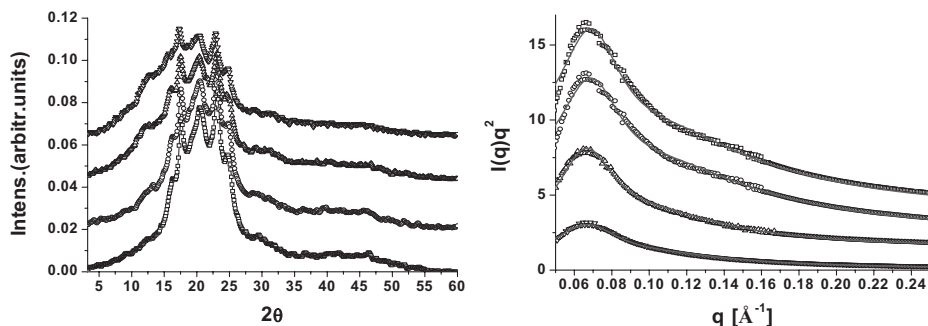


Figure 4.

The comparison of: WAXS patterns (left side) and desmeared Lorentz corrected SAXS curves (right side) of blends as prepared and the BTA reference sample (the curves are vertically shifted for clarity); ▽ = BTA; - = BTA90/PLA10; 8 = BTA70/PLA30; X = BTA50/PLA50; — = fitted Hosemann scattering function.

Table 1.
The data of the heating induced changes of BT-BA domains structure.

BTA/PLA	an ambient temperature				heating		just before melting			
	$\langle d_1 \rangle$	$\langle d_2 \rangle$	$\langle L \rangle$	φ	τ^a	τ_L^b	$\langle d_1 \rangle$	$\langle d_2 \rangle$	$\langle L \rangle$	φ
	Å	Å	Å	%	K	K	Å	Å	Å	%
100/0	63.0	12.5	75.5	17.0	65	46	129.0	26.0	155.0	17.0
90/10	62.0	14.0	76.0	18.0	65	45	132.0	25.0	157.0	16.0
70/30	61.0	20.0	81.0	26.0	44	38	149.0	24.0	173.0	13.0
50/50	58.0	18.0	76.0	24.0	29	28	156.0	24.0	180.0	13.5

^{a)}the constant of an exponential growth of the $\langle d_1 \rangle$ amorphous layers thickness.
^{b)}the constant of an exponential growth of the $\langle L \rangle$ long period of BT-BA stacks.

Figure 4 right side) that for all the blends a single small-angle scattering maximum is observed at ca. the same position as for BTA reference sample, however the intensity of the maximum decreases systematically in the decrease of BTA content. Assuming that the scattering maximum originates in BT-BA lamellar stacks^[11] included within the blends, the characteristics of an initial lamellar superstructure of BT-BA semicrystalline domains within the blends (as well as in BTA reference sample) have been derived from fitting of the Hosemann scattering function (Eqs. 3) to the desmeared Lorentz corrected SAXS curves. In general, results of this analysis show (data collected in Table 1) that BT-BA lamellar stacks before the thermal cyclic treatment of the samples were

composed of relatively thin BT crystalline layers ($\langle d_2 \rangle \approx 12 \div 20$ Å) and much thicker BA amorphous layers ($\langle d_1 \rangle \approx 63 \div 61$ Å). Consequently, the $\langle L \rangle$ long period of the BT-BA lamellar stacks was estimated at ca.: $75 \div 81$ Å, and the φ volume fraction of BT crystalline layers within the stacks ($\varphi = \langle d_2 \rangle / \langle L \rangle$) was estimated at ca.: $17 \div 26\%$. It should be underlined that the level of φ values obtained from the SAXS analysis corresponds well with the level of WAXS derived crystallinity for the BTA reference sample (22%).

The structure behavior during the heating/cooling cycle treatment (see Figure 2) of: the BTA copolyester and the BTA/PLA-b blends has been examined by time resolved SAXS measurements. The collections of Lorentz corrected SAXS curves

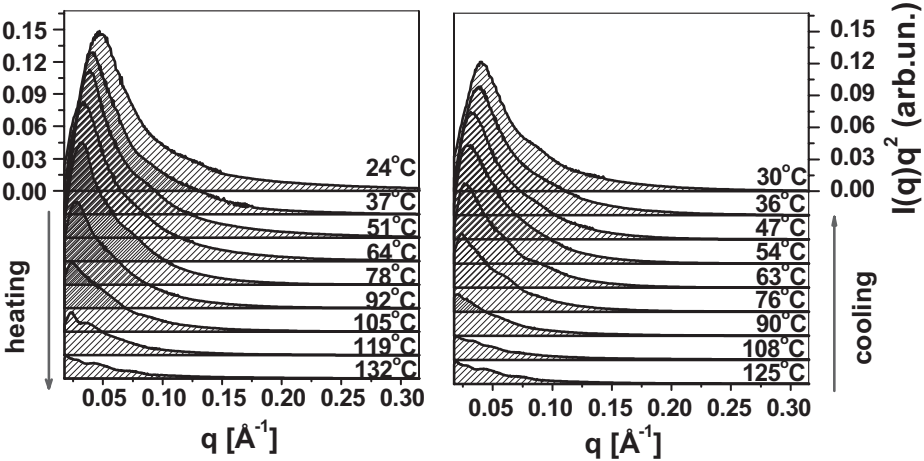


Figure 5.
The collection of desmeared Lorentz corrected SAXS curves determined for the step-heated (left side) and subsequently continuous-cooled (right side) BTA70/PLA30 blend.

determined for the BTA70/PLA30 blend are presented in Figure 5, as a representative example. In the left side figure a systematic shift of the SAXS maximum towards smaller q values and a systematic decrease of the SAXS maximum intensity are observed along with the increase of temperature of the heated sample. In the figure right side, opposite changes of the SAXS maximum are observed along with the decrease in the temperature of the sample, beginning from the forth SAXS curve determined for the cooled sample. Similar changes in temperature SAXS curves of the other BTA/PLA-b blends and the BTA copolyester were observed except that the SAXS maximum appeared again on the third SAXS curve determined during the cooling of both the BTA copolyester and the BTA90/PLA10 blend. This difference indicates that during the cooling of the melted blends: BTA70/PLA30 and BTA50/PLA50 primary and well formed BT-BA stacks appear again significantly later and thereby at lower temperature (i.e. ca. 5 min. later and at ca. 15 °C lower temperature) than during the cooling of melted: BTA copolyester and BTA90/PLA blend. Results obtained from the fitting of the Hosemann scattering function to temperature SAXS curves of the samples (except results obtained for the BTA90/PLA10 blend) are presented in Figures 6 ÷ 8, and the data of global structure changes of the samples is compared in Tables 1 and 2.

Figure 6 shows changes in: the Q_{exp} scattering power, the $\langle d_1 \rangle$ thickness of BA amorphous layers, the $\langle d_2 \rangle$ thicknesses of BT crystalline layers, and the $\langle L \rangle$ long period of BT-BA stacks vs. temperature of a

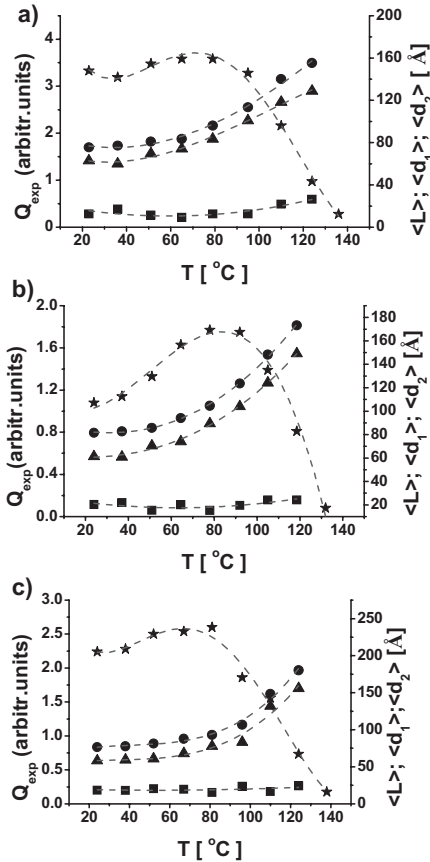


Figure 6. The heating induced changes of characteristics of BTA domains of: a) the BTA copolyester, b) the BTA70/PLA30 blend and c) the BTA50/PLA50 blend; ξ = the Q_{exp} scattering power; $\langle L \rangle$ = the long period; $\langle d_1 \rangle$ = the amorphous layers thickness; $\langle d_2 \rangle$ = the crystalline layers thickness.

step-heated sample of: a) the BTA copolyester, b) the BTA70/PLA30 blend and c) the BTA50/PLA50 blend. First of all, one can notice that a course of changes in individual characteristics is similar for all the samples.

Table 2. The data of a course of structure changes during the cooling.

BTA/PLA	t_0 ^{a)} min.	$\langle T_0 \rangle$ ^{a)} °C	t_f min.	Δt_f mi.	T_f °C	$\langle d_1 \rangle_{60}$ Å	$\langle d_2 \rangle_{60}$ Å	$\langle L \rangle_{60}$ Å	Φ_{60} %
100/0	10 ÷ 15	94	18.5	6.6	82.0	86.5	25.0	111.5	22.5
90/10	10 ÷ 15	95	18.0	6.5	82.0	85.0	25.0	110.0	23.0
70/30	15 ÷ 20	76	16.5	4.4	92.0	69.5	25.0	94.5	26.0
50/50	15 ÷ 20	78	15.0	7.7	92.0	70.5	20.5	91.0	22.5

^{a)} t_0 , $\langle T_0 \rangle$ - respectively: the cooling time and temperature of the appearance again of BT-BA stacks.

The Q_{exp} scattering power increases initially in the range from ca. 40 °C to 80 °C and then it drops drastically in the range from ca. 80 °C to 130 °C. In general, scattering power of small angle X-ray scattering depends on^[1]: a squared electron density contrast between phases of a given system and a product of the phases volume fraction. So, the drop of the Q_{exp} originates in a systematic disappearance of the lamellar superstructure of BTA domains. It is interesting to note that the rate of the lamellar superstructure disappearance is highest for the BTA70/PLA30 blend as it is indicated by a slope of the Q_{exp} curves in the temperature range of the Q_{exp} drop.

In the case of the $\langle L \rangle$ long period and the $\langle d_1 \rangle$ amorphous layers thickness regular growth is observed in the whole temperature range of the heating, resulting finally in the increase in: the $\langle L \rangle$ from ca. 75÷80 Å up to 155÷185 Å and the $\langle d_1 \rangle$ from ca. 60 Å up to 130÷155 Å. Thus, changes in the $\langle d_2 \rangle$ crystalline layers thickness around the level of 12÷26 Å are of minor significance for the double increase of $\langle L \rangle$. To estimate the rate of the heating induced growth of both the $\langle L \rangle$ and the $\langle d_1 \rangle$ the experimental curves of these characteristics have been fitted by an exponential function: $y = y_0 + A \exp(T/\tau)$, where τ is a temperature constant of a growth. The values determined for the τ constant (see Table 1) clearly show that the growth rate of the $\langle d_1 \rangle$ amorphous layers thickness and consequently of the $\langle L \rangle$ long period of BT-BA stacks significantly increases with the increase of the PLA-b content in the blends.

The 2D plots in Figures 7 and 8 show respectively changes in: the $\langle L \rangle$ long period and the Q_{exp} scattering power as a function of both the cooling time (t) and the $\langle T \rangle$ temperature (see Eqs. 1) of the cooled BTA copolyester and of the cooled blends: BTA70/PLA30 and BTA50/PLA50. For all the samples the $\langle L \rangle$ long period of BT-BA stacks decreases as could be expected with the increase of the cooling time and the decrease of the temperature, but the changes of the $\langle L \rangle$ are more or less

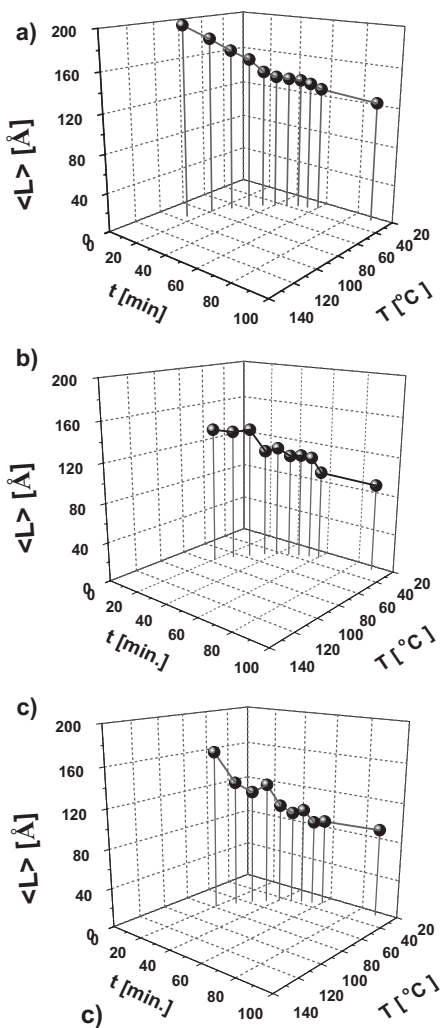


Figure 7.

2D plots of changes of the $\langle L \rangle$ long period for a cooled sample of: a) the BTA copolyester, b) the BTA70/PLA30 blend and c) the BTA50/PLA50 blend.

irregular for the blends whereas they are very regular for the BTA copolyester. Finally, at the end of the 60 minute cooling the $\langle L \rangle$ long period as well as the: $\langle d_1 \rangle$ and $\langle d_2 \rangle$ thicknesses respectively of: the BA amorphous and BT crystalline layers are significantly bigger than before the cycle treatment of the samples (compare the data given in Table 2 and 1).

The Q_{exp} curves look like a sigmoidal course, limited by a scattering power of a given sample respectively: at its melt state

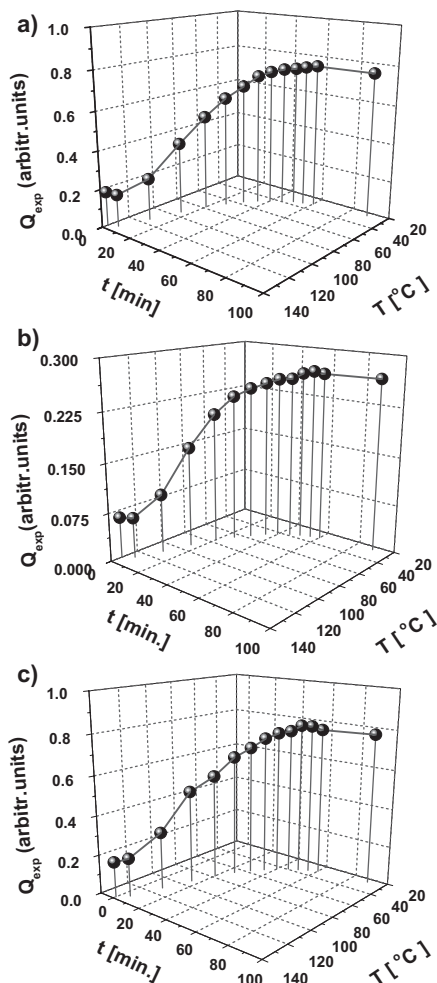


Figure 8.

2D plots of changes of the Q_{exp} scattering power for a cooled sample of: a) the BTA copolyester, b) the BTA70/PLA30 blend and c) the BTA50/PLA50 blend.

(achieved at the end of the heating) and at its condense state (achieved at the end of the subsequent cooling). The changes of the Q_{exp} as a function of the cooling time were analysed using a Boltzmann sigmoidal function. As a result, the centre (t_f) of fastest changes of the Q_{exp} and a range time (Δt_f) around the t_f of the fastest changes have been determined in the cooling time scale. The data of the t_f centre and the Δt_f range is collected in Table 2.

In fact, the values of the t_f time show that most rapid structural changes appeared

significantly earlier for the BTA/PLA-b blends than for BTA copolyester (i.e. ca. $2 \div 3$ minutes earlier) and thereby at higher temperature (at ca. 10°C). On the other hand, the reverse relation has been affirmed between the beginning of the appearance of BT-BA lamellar stacks in the cooled blends and in the cooled BTA copolyester. This discrepancy indicates that most probably a formation of PLA-b amorphous domains starts relatively early during the cooling of the melted blends and resulting in an initial increase of the Q_{exp} and that the primary PLA domains hinder and slow down the formation of BT-BA stacks. The Δt_f range can be considered a measure of duration of most rapid structural changes occurring during the cooling of the melted samples. In accordance with the data of the Δt_f range the duration of the structural changes was shortest for the BTA70/PLA30 blend. It is worth to underline that this observation corresponds well with the behavior of the samples during the heating. In that case (see Figure 6) the rate of the structural changes which occurred in the temperature range of the melting was biggest for the BTA70/PLA30 blend as well.

Conclusion

In summary, we have reported the characterization of both the phase structure of the biodegradable BTA/PLA-b blends as prepared as well as structure changes occurred during the step-heating/continuous-cooling cycle treatment ($20 \div 135 \div 20^\circ\text{C}$) of the blends and linked results obtained with structure changes determined for BTA reference sample treated in the same way.

The following main conclusions can be drawn from the data obtained using X-ray methods:

- the phase structure of the blends consists of: PLA-b amorphous phase, BT crystalline phase and BA amorphous phase,
- the BT-BA semicrystalline domains included in the blends exhibit lamellar superstructure and the mean thicknesses

- of both BA amorphous and BT crystalline layers (ca. $58 \div 62$ Å and $14 \div 20$ Å respectively) of the BT-BA stacks are close to the mean thicknesses of the layers of lamellar superstructure of the BTA copolyester,
- the SAXS derived volume fraction of BT crystalline layers in the BT-BA stacks included in the blends as prepared is equal to ca. $18 \div 26\%$ and does not differ significantly from the SAXS derived volume fraction of the BT crystalline layers for the BTA copolyester,
 - the heating induced changes of the mean long period of BT-BA stacks consist mainly of the thickening of BA amorphous layers and the bigger changes rate, the bigger the PLA-b polylactide amount is,
 - the disappearance of the lamellar structure of BT-BA domains in the temperature range of melting happens fastest for the blend with the 30%wt amount of the polylactide
 - the BT-BA stacks appear again significantly later and thereby at lower temperature (ca. 5 min and ca. 15°C respectively) during the cooling of the melted blends with the higher amount of PLA-b (30 and 50% wt) than during the cooling of the melted BTA copolyester, whereas the most rapid structural changes occur significantly earlier and thereby at higher temperature (ca. $2 \div 3$ min and ca. 10°C respectively) during the cooling of the melted blends than during the cooling of the melted BTA copolyester
 - the duration of the most rapid structural changes ranges from ca. 5 to 8 minutes and it is shortest for the blend with 30% wt amount of PLA-b
 - at the end of the 60 minute cooling the mean thickness of the amorphous and crystalline layers of the BT-BA stacks and consequently the mean long period of the stacks structure are considerably bigger (ca. x%) with reference to the initial state before the cycle treatment.

[1] M. A. Singh, S. W. S. Gosh, R. F. Shannon, *J. Appl. Cryst.* **1993**, 26, 787.

[2] W. Weigand, W. Ruland, *Prog. Colloid Polym. Sci.* **1979**, 66, 335.

[3] G. Porod, in: "Small Angle X-ray Scattering", 2nd ed., O., Glatter, O. Kratky, Eds., Academic Press, New York **1982**, p. 17.

[4] C. G. Vonk, in: "Small Angle X-ray Scattering", 2nd ed., O., Glatter, O. Kratky, Eds., Academic Press, New York **1982**, p. 433.

[5] R. Hosemann, *Z. Phys.* **1949**, 127, 16.

[6] R. Hosemann, S. N. Bagchi, "Direct analysis of diffraction by matter", North-Holland Publishing Co. Amsterdam, **1962**.

[7] K. Kuwabara, Z. Gan, T. Nakamura, H. Abe, Y. Doi, *Biomacromol.* **2002**, 3, 390.

[8] E. Cranston, J. Kawada, S. Raymond, F. G. Morin, R. H. Marchessault, *Biomacromol.* **2003**, 4, 995.

[9] Z. Gan, K. Kuwabara, M. Yamamoto, H. Abe, Y. Doi, *Polym. Degrad. Stab.* **2004**, 83, 289.

[10] Z. Gan, K. Kuwabara, H. Abe, T. Iwata, Y. Doi, *Biomacromol.* **2004**, 5, 371.

[11] X. Q. Shi, H. Ito, T. Kikutani, *Polymer* **2005**, 46, 11442.

[12] J. Blomqvist, B. Mannfors, L. O. Pietila, *Polymer* **2002**, 43, 4571.